

Short Papers

Statistical Estimation and Testing for Variation Root-Cause Identification of Multistage Manufacturing Processes

Shiyu Zhou, Yong Chen, and Jianjun Shi

Abstract—Root-cause identification for quality-related problems is a key issue in quality and productivity improvement for a manufacturing process. Unfortunately, root-cause identification is also a very challenging engineering problem, particularly for a multistage manufacturing process. In this paper, root-cause identification is formulated as a problem of estimation and hypothesis testing of a general linear mixed model. First, a linear mixed fault-quality model is built to describe the cause-effect relationship between the process faults and product quality. Then, the estimation algorithms developed for a general linear mixed model are adapted to estimate the process mean and variance. Finally, a hypothesis testing method is developed to determine if process faults exist in terms of statistical significance. A detailed experimental study illustrated the effectiveness of the proposed methodology.

Note to Practitioners—Economic globalization brings intense competition among manufacturing enterprises. The key to succeed in this competitive climate is to rapidly respond to fast-changing market demands with high-quality and competitively priced products. To achieve this, we need to quickly identify root causes of quality-related problems in a complicated manufacturing system. However, the current widely adopted quality-control techniques focus more on monitoring than on root-cause identification. These techniques can efficiently detect the changes in the process but the root cause identification is often left to the plant engineers or operators. In this paper, a systematic estimation and testing method is proposed to identify the variational root causes in multistage manufacturing processes. First, a linear model is built based on the design information to describe the cause-effect relationship between the process faults and product quality. Then, an algorithm is developed to estimate the mean and variance of the process faults from the quality measurements of products. Finally, a statistical testing method is developed to determine if process faults (i.e. root causes) exist in terms of statistical significance. A detailed experimental study illustrates the effectiveness of this method. The method presented in this paper is a new quality-control technique and can be used for quality improvement of multistage manufacturing processes.

Index Terms—Linear mixed model, multistage manufacturing process, root-cause identification, variation propagation.

I. INTRODUCTION

Root-cause identification for quality-related problems is a key and necessary step for the operation of manufacturing processes, especially the high-throughput automated processes. Root-cause identification is also a challenging engineering problem. This is particularly true for the multistage manufacturing processes, which is defined as a process that

Manuscript received January 9, 2003; revised June 24, 2003. This work was supported by the National Science Foundation Engineering Research Center for Reconfigurable Machining Systems under NSF Grant EEC95-92125 and NSF Grant DMI-0322147.

S. Zhou is with the Department of Industrial Engineering, University of Wisconsin-Madison, Madison, WI 53706 USA (e-mail: szhou@enr.wisc.edu).

Y. Chen is with the Department of Mechanical and Industrial Engineering, The University of Iowa, Iowa City, IA 52242 USA (e-mail: yongchen@engineering.uiowa.edu).

J. Shi is with the Department of Industrial and Operations Engineering, The University of Michigan, Ann Arbor, MI 48109 USA (e-mail: shihang@umich.edu).

Digital Object Identifier 10.1109/TASE.2004.829427

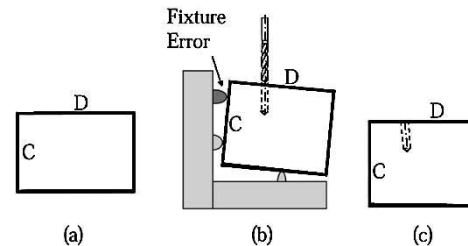


Fig. 1. Effect of fixture error.

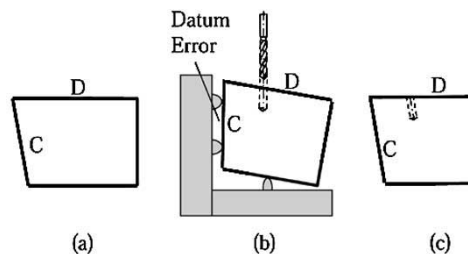


Fig. 2. Effect of datum error.

produces the products under multiple setups. The quality information flow of the product in a multistage manufacturing system and the interaction between the process faults and the product quality characteristics are very complicated. The effect of certain process fault on the product quality could propagate along the process, and different process faults could have the same manifestation on the product quality. An example of a two-stage machining process is shown in Figs. 1 and 2.

The workpiece is a cube of metal (the front view is shown). Surface C of the workpiece is milled in the first step [Fig. 1(a)]. The hole is drilled in surface D in the second step [Fig. 1(b)]. Due to an error in the locating pins of the fixture in the second step, the resulting hole is not perpendicular to surface D, as shown in Fig. 1(c). In this example, the perpendicularity of the hole is the product quality characteristic and the quality-related problem is caused by the fixture error, so-called “root cause” or “process fault.” In most cases, the process root causes are not directly measurable and have to be identified based on product quality measurements. For a multistage process, the identification is not straightforward. For example, in the process illustrated in Fig. 2, the resulting hole is not perpendicular to surface D [Fig. 2(c)] either. However, the root cause is not the fixture error in the second drilling step [Fig. 2(b)]. Instead, the root cause is the process fault in the first milling operation [Fig. 2(a)]. In other words, the process faults in a multistage process might propagate along the process to the downstream stages. This paper focuses on a systematic method of root-cause identification using product quality data of multistage machining processes.

Statistical process control (SPC) [1], [2] is the main technique frequently used in practice for process quality control. In the SPC scheme, measurements of product quality characteristics are taken from the finished or intermediate product, and they are treated as random variables. The key parameters of their statistical distribution such as the mean value and variance are compared with those under normal conditions. If the differences are larger than pre-specified thresholds, an alarm is generated to indicate that some changes happen in the process. Although

the SPC method can detect the process change, it cannot pinpoint the fault or root cause of the change. The root-cause identification is left to the plant engineers or operators.

With the fast development of information technology, an abundance of product quality measurement information is readily available. For example, optical coordinate measurement machines (OCMM) are commonly installed at multiple locations in a multistage automotive body assembly process to obtain the dimensional measurement of the assembled product [3]. In metal cutting processes, the inline probing capability at certain key stages is commonly available as well [4]. This abundant product measurement information provides great opportunities not only for quality monitoring and assurance, but also for root-cause identification.

Recently, some research work on root-cause identification based on product quality measurements has been reported. The research work can be put into two categories: the single-stage case and the multistage case. For the single stage case, Ceglarek and Shi [5] studied the fixture fault diagnosis in the automotive body assembly under the rigid part and single fault assumption. Their method is extended in [6] to the compliant beam structure assembly model. Chang and Gossard [7] used computer simulation to generate a model that relates the process faults with the product dimensional variation. Then linear optimization and statistical techniques are employed to determine the process faults. Apley and Shi [8] presented a more general fixture diagnostic methodology for panel assembly. In their work, least-squares estimation and the statistical hypothesis testing procedure are used to identify the fixture fault based on the product measurement data. Their work still concentrates on a single-stage process.

From the above literature, we can see that two basic elements exist in root-cause identification: a mathematical model (preferable linear) that links the process fault and the product quality measurement, and a fault mapping procedure based on this model. Most recently, some researchers developed several mathematical models that describe the quality information flow in multistage manufacturing processes, including assembly processes [9]–[12] and machining processes [13]–[15]. These fault-quality modeling techniques provide opportunities for the development of root-cause identification in multistage manufacturing processes.

Ding *et al.* [16] proposed a fixture error diagnosis technique for the multistage assembly process based on a state–space model. Their techniques can only be used to detect a single fault in the system. Zhou, *et al.* [17] and Ding *et al.* [18] studied the diagnosability issues for the root-cause identification of a multistage manufacturing process. Based on the theory of general linear mixed model, a concept of minimal diagnosable class is proposed to describe the system diagnosability. Ding *et al.* [19] further summarized and compared the variation estimation algorithms used for linear mixed models. No discussion on the confidence level of the estimation results is presented in their paper.

This paper presents a methodology and an experimental study of the root-cause identification for multistage machining processes. A mathematical model that links the process faults (e.g., the error of the locating pin) and the product quality measurements is first built. This model can be viewed as a linear mixed model. Hence, multiple process faults can be estimated simultaneously using point estimation algorithms for linear mixed models. Finally, a hypothesis-testing procedure is developed to provide confidence level of the estimation results. To illustrate the methodology, an experimental study of a multistage machining process is presented in detail.

This paper is organized as follows. The problem formulation and estimation algorithms are presented in Section II. The proposed hypothesis testing method is discussed in Section III. The experimental study

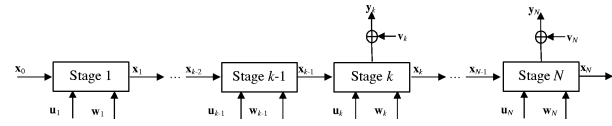


Fig. 3. Diagram of a multistage manufacturing process.

and analysis are presented in Section IV. This paper is concluded in Section V.

II. ESTIMATION OF PROCESS FAULTS IN MULTISTAGE MACHINING PROCESSES

A. Fault-Quality Modeling of Multistage Machining Processes

A multistage machining process can be represented by the diagram in Fig. 3.

Those symbols in Fig. 3 are explained as follows.

- The product quality information (i.e., the part dimensional deviations) at each stage is represented by the state vector \mathbf{x}_k . In more detail, “vectorial representation” of a part, which conforms to the working principles of the coordinate measurement machine (CMM) and computer-aided design/computer-aided modeling (CAD/CAM) models, is adopted to describe the dimensional deviation of the product features [20].
- The process faults (e.g., the fixture error, machining error, or thermal errors in machining processes, etc.) are treated as system inputs \mathbf{u}_k . *The process faults or root causes manifest themselves as a shift of the mean value of \mathbf{u}_k and/or an increase of the variance of \mathbf{u}_k .* This definition of process fault is consistent with the most common concerns in the process quality control. The components of \mathbf{u}_k are assumed independent of each other.
- The process unmodeled errors are represented by a noise input to the system \mathbf{w}_k . We assume that \mathbf{w}_k is zero mean and the components of \mathbf{w}_k are independent of each other. Further, \mathbf{w}_k is independent of \mathbf{u}_i , $i = 1, \dots, N$. Under the small-error assumption, \mathbf{w}_k contains a second order or a higher order of small values. Hence, the magnitude of \mathbf{w}_k is quite small comparing with \mathbf{x}_k and \mathbf{u}_k .
- The measurements of product quality deviation are denoted by \mathbf{y}_k . Please note that \mathbf{y}_k is not necessarily available at every stage.
- The measurement noise is denoted by a zero mean random vector \mathbf{v}_k . The components of \mathbf{v}_k are independent with each other. Further, \mathbf{v}_k is independent of \mathbf{u}_i , \mathbf{w}_i , and \mathbf{x}_i , $i = 1, \dots, N$.

Using the small error assumption, a linear state–space model can be built to describe the product quality information flow as follows:

$$\begin{aligned}\mathbf{x}_k &= \mathbf{A}_{k-1}\mathbf{x}_{k-1} + \mathbf{B}_k\mathbf{u}_k + \mathbf{w}_k \\ \mathbf{y}_k &= \mathbf{C}_k\mathbf{x}_k + \mathbf{v}_k\end{aligned}\quad (1)$$

where $\mathbf{A}_{k-1}\mathbf{x}_{k-1}$ represents the quality information transformation from the $(k-1)$ th stage to the k th stage, $\mathbf{B}_k\mathbf{u}_k$ represents the part quality affected by the process faults, \mathbf{C}_k is the measurement matrix that maps the product quality characteristics to the measurements. System matrices \mathbf{A}_k , \mathbf{B}_k , and \mathbf{C}_k are constant matrices. They are determined by the process/product design, or, in other words, these matrices include the interaction information between the process and the product. The detailed derivation and validation of the model can be found in [13].

The complicated variation propagation is handled automatically in this model through the state transition. To construct this model, we only need to study locally the relationship among \mathbf{x}_{k-1} , \mathbf{x}_k , and \mathbf{u}_k at

each individual stage k . Hence, the large body of knowledge about the single-stage operation can be readily reused in the model construction.

The state–space model (1) provides a quantitative framework for variation propagation analysis, diagnosis, and control in complicated multistage processes. Although (1) is in the state–space form, there are some significant differences between this model and the state–space model used in the dynamic control field [21].

- 1) In (1), the index k represents the stage number rather than time. Comparing with the time index, the stage index is always limited in a multistage process.
- 2) The main objective of using (1) is to estimate *the mean and the variance* of the input to the system \mathbf{u}_k based on the output \mathbf{y}_k ; in control theory, on the other hand, the control inputs are often known and the objective is to estimate and control the states \mathbf{x}_k .

These differences make it difficult to apply the estimation techniques in control theory literature such as the Kalman filter method [22]. Instead, the statistical-estimation techniques for the linear mixed model can be used as illustrated in the following sections.

B. Formulation of the Root-Cause Identification Problem

The state–space model in (1) can be transformed into a linear input–output model as follows. First, it can be written as

$$\mathbf{y}_k = \sum_{i=1}^k \mathbf{C}_k \Phi_{k,i} \mathbf{B}_i \mathbf{u}_i + \mathbf{C}_k \Phi_{k,0} \mathbf{x}_0 + \sum_{i=1}^k \mathbf{C}_k \Phi_{k,i} \mathbf{w}_i + \mathbf{v}_k \quad (2)$$

where $\Phi_{(\cdot,\cdot)}$ is the state transition matrix, $\Phi_{k,i} = \mathbf{A}_{k-1} \mathbf{A}_{k-2} \cdots \mathbf{A}_i$ for $k > i$ and $\Phi_{k,k} = \mathbf{I}$. \mathbf{x}_0 corresponds to the initial condition of the product before it goes into the manufacturing line. If the measurement of \mathbf{x}_0 is available, the term $\mathbf{C}_k \Phi_{k,0} \mathbf{x}_0$ can be moved to the left-hand side of (2) and $\mathbf{y}_k - \mathbf{C}_k \Phi_{k,0} \mathbf{x}_0$ can be treated as a new measurement. If \mathbf{x}_0 is not available, we can treat it as an additional process fault input. Without loss of generality, we can set \mathbf{x}_0 to 0.

The process faults and input \mathbf{u}_i often manifest themselves as the shift of the mean value and the increase of variances. For example, consider the fixture error in a machining or assembly process. The locator position of the fixture system could have a very slow drifting due to wear. This error can be viewed as a mean shift of the locating position. On the other hand, the locator position could have a random variation if it is loosened. This error can be viewed as a variance increase of the locating position. For the purpose of root-cause identification, we need to identify both *the mean and the variance* of the fault inputs. To do so, \mathbf{u}_i is split into a constant part $\boldsymbol{\mu}_i$ and a zero-mean random part $\tilde{\mathbf{u}}_i$ as follows.

Define

$$\boldsymbol{\gamma}_{ki} = \begin{cases} \mathbf{C}_k \Phi_{k,i} \mathbf{B}_i, & k \geq i \\ \mathbf{0}, & k < i \end{cases} \quad \boldsymbol{\beta}_{ki} = \begin{cases} \mathbf{C}_k \Phi_{k,i}, & k \geq i \\ \mathbf{0}, & k < i \end{cases} \boldsymbol{\mu}_i$$

as the expectation of \mathbf{u}_i , and $\tilde{\mathbf{u}}_i = \mathbf{u}_i - \boldsymbol{\mu}_i$, (2) can be rewritten as

$$\mathbf{y}_k = \sum_{i=1}^N \boldsymbol{\gamma}_{ki} \boldsymbol{\mu}_i + \sum_{i=1}^N \boldsymbol{\gamma}_{ki} \tilde{\mathbf{u}}_i + \sum_{i=1}^N \boldsymbol{\beta}_{ki} \mathbf{w}_i + \mathbf{v}_k \quad (3)$$

where $\boldsymbol{\mu}_i$ is a constant vector and $\tilde{\mathbf{u}}_i$, \mathbf{w}_i , \mathbf{v}_k are uncorrelated random vectors with zero means.

During the production, multiple samples of the product are available. Denote vector \mathbf{y}_{ki} as the i th sample of the dimensional quality characteristics at the k th stage, $\tilde{\mathbf{U}}_i^T = [\tilde{u}_{1i}^T \cdots \tilde{u}_{ki}^T \cdots \tilde{u}_{Ni}^T]$, $\mathbf{W}_i^T = [\mathbf{w}_{1i}^T \cdots \mathbf{w}_{ki}^T \cdots \mathbf{w}_{Ni}^T]$, $\boldsymbol{\Gamma}_k = [\boldsymbol{\gamma}_{k1} \cdots \boldsymbol{\gamma}_{kk} \cdots \boldsymbol{\gamma}_{kN}]$, $\boldsymbol{\Psi}_k = [\boldsymbol{\beta}_{k1} \cdots \boldsymbol{\beta}_{kk} \cdots \boldsymbol{\beta}_{kN}]$, $\mathbf{U}^T = [\boldsymbol{\mu}_1^T \cdots \boldsymbol{\mu}_k^T \cdots \boldsymbol{\mu}_N^T]$, \mathbf{v}_{ki}

as the measurement noise at the k th stage for the i th sample; then, (3) can be written in a matrix form for the i th sample

$$\mathbf{y}_{ki} = \boldsymbol{\Gamma}_k \mathbf{U} + [\boldsymbol{\Gamma}_k \quad \boldsymbol{\Psi}_k] \begin{bmatrix} \tilde{\mathbf{U}}_i \\ \mathbf{W}_i \end{bmatrix} + \mathbf{v}_{ki}. \quad (4)$$

Denote P as the total number of potential faults (the dimension of \mathbf{U}) and Q as the total number of process noise considered on all the stages (the dimension of \mathbf{W}_i), $\{\sigma_{u_i}^2\}_{i=1,\dots,P}$, $\{\sigma_{w_j}^2\}_{j=1,\dots,Q}$, and σ_v^2 are the variances of the elements of $\tilde{\mathbf{U}}_i$, the variances of the elements of \mathbf{W}_i , and the variance of the observation noise, respectively. They are also called variance components.

Collecting all the measurements on all the stages as $\mathbf{Y}_i^T = [\mathbf{y}_{1i}^T \cdots \mathbf{y}_{ki}^T \cdots \mathbf{y}_{Ni}^T]$, and denote $\boldsymbol{\Upsilon}^T = [\boldsymbol{\Gamma}_1^T \cdots \boldsymbol{\Gamma}_k^T \cdots \boldsymbol{\Gamma}_N^T]$, $\boldsymbol{\Phi}^T = [\boldsymbol{\Psi}_1^T \cdots \boldsymbol{\Psi}_k^T \cdots \boldsymbol{\Psi}_N^T]$, and $\mathbf{V}_i^T = [\mathbf{v}_{1i}^T \cdots \mathbf{v}_{ki}^T \cdots \mathbf{v}_{Ni}^T]$. We further have

$$\mathbf{Y}_i = \boldsymbol{\Upsilon} \mathbf{U} + [\boldsymbol{\Upsilon} \quad \boldsymbol{\Phi}] \begin{bmatrix} \tilde{\mathbf{U}}_i \\ \mathbf{W}_i \end{bmatrix} + \mathbf{V}_i. \quad (5)$$

Equation (5) can be stacked up to represent multiple samples. For M samples, denote $\mathbf{Y}^T = [\mathbf{Y}_1^T \cdots \mathbf{Y}_i^T \cdots \mathbf{Y}_M^T]$, $\boldsymbol{\Gamma}^T = [\boldsymbol{\Upsilon}^T \cdots \boldsymbol{\Upsilon}^T \cdots \boldsymbol{\Upsilon}^T]$, $\mathbf{V}^T = [\mathbf{V}_1^T \cdots \mathbf{V}_i^T \cdots \mathbf{V}_M^T]$

$$\mathbf{W}^T = \begin{bmatrix} \mathbf{W}_1^T & \cdots & \mathbf{W}_i^T & \cdots & \mathbf{W}_M^T \end{bmatrix}$$

$$\mathbf{Z}^{(1)} = \begin{bmatrix} \boldsymbol{\Upsilon} & & & & \\ & \ddots & & & \\ & & \boldsymbol{\Upsilon} & & \\ & & & \ddots & \\ & & & & \boldsymbol{\Upsilon} \end{bmatrix}$$

$$\mathbf{Z}^{(2)} = \begin{bmatrix} \boldsymbol{\Phi} & & & & \\ & \ddots & & & \\ & & \boldsymbol{\Phi} & & \\ & & & \ddots & \\ & & & & \boldsymbol{\Phi} \end{bmatrix}$$

$$\tilde{\mathbf{U}}^T = \begin{bmatrix} \tilde{\mathbf{U}}_1^T & \cdots & \tilde{\mathbf{U}}_i^T & \cdots & \tilde{\mathbf{U}}_M^T \end{bmatrix}$$

the fault-quality model for M samples is

$$\mathbf{Y} = \boldsymbol{\Gamma} \mathbf{U} + [\mathbf{Z}^{(1)} \quad \mathbf{Z}^{(2)}] \begin{bmatrix} \tilde{\mathbf{U}} \\ \mathbf{W} \end{bmatrix} + \mathbf{V}. \quad (6)$$

Equation (6) is a static linear model. However, this model is different from the conventional multivariate regression model such as $\mathbf{Y} = \mathbf{X}\boldsymbol{\beta} + \boldsymbol{\varepsilon}$. In regression analysis, the main objective is to estimate the constant $\boldsymbol{\beta}$ under the disturbance of $\boldsymbol{\varepsilon}$. However, in (6), besides the constant \mathbf{U} , we also need to estimate the variances of $\tilde{\mathbf{U}}$ because the variance change of the process variables is also an important process fault. This difference makes it difficult to directly apply the regression techniques such as the ordinary least-squares method [23] and robust estimation method for linear models [24], [25] to solve this problem.

Equation (6) is actually in the format of a linear mixed model that has been studied in biological and agricultural research [26], [27]. In the terminology of the linear mixed model, \mathbf{U} is the *fixed effect*, $\begin{bmatrix} \tilde{\mathbf{U}} \\ \mathbf{W} \end{bmatrix}$ is the *random effect*, $\boldsymbol{\Gamma}$ and $[\mathbf{Z}^{(1)} \quad \mathbf{Z}^{(2)}]$ are the *design matrices*, and \mathbf{V} is the *residual error*. Several techniques have been developed to solve the estimation problem in linear mixed model: from M samples of quality measurements, how can we identify the mean and the variance of the process faults, $\{\boldsymbol{\mu}_i\}_{i=1,\dots,P}$ and $\{\sigma_{u_i}^2\}_{i=1,\dots,P}$, respectively? This problem is exactly the root-cause identification problem we are facing.

C. Estimation of the Root Causes

A large body of literature exists regarding the estimation of the fixed and random effects of a linear mixed model. A comparison study of these methods can be found in [19]. The typical statistical estimation algorithms are ANOVA, maximum likelihood estimation (MLE), restricted maximum likelihood estimation (REML), and minimum norm quadratic unbiased estimation (MINQUE). Excellent reviews of these methods can be found in [26]. In general, the ANOVA-type estimation method cannot be applied to the complicated general linear mixed model as in (6). MLE and REML are powerful estimation methods that maximize the likelihood function of the observed data for a given specified form of joint distribution of the observations. However, the computational load of ML or REML method is high. MINQUE tries to minimize a quadratic norm defined in [28]. It can be proved that MINQUE solution can be obtained by one step iteration of the ML equations with a pre-assigned initial value [27]. Hence, the computational load of MINQUE is much lower than that of ML or REML.

One of the focuses of this article is to develop a hypothesis testing method to provide confidence level of the root-cause identification, instead of just providing an estimation of the process faults. Therefore, it is preferable to select an estimation method of which the statistical properties of the estimation results (i.e., the estimated mean and variance) are known. It is well known that ML estimator possesses very good characteristics such as consistency, asymptotic normality, and efficiency. Hence, the ML estimator will be used in this paper. MINQUE, as an approximation of the ML method, will also be used.

The ML method for the fault-quality model (6) is given as follows:

$$\boldsymbol{\mu}_Y \equiv E(\mathbf{Y}) = \boldsymbol{\Gamma}\mathbf{U} \quad (7)$$

$$\boldsymbol{\Sigma}_Y \equiv \text{Cov}(\mathbf{Y}) = \mathbf{F}_1\sigma_{u_1}^2 + \cdots + \mathbf{F}_P\sigma_{u_P}^2 + \mathbf{F}_{P+1}\sigma_{w_1}^2 + \cdots + \mathbf{F}_{P+Q}\sigma_{w_Q}^2 + \mathbf{F}_{P+Q+1}\sigma_v^2 \quad (8)$$

where $E(\cdot)$ represents the expectation, $\text{Cov}(\cdot)$ represents the covariance matrix of a random vector, and

$$\mathbf{F}_i = \begin{cases} \sum_{k=1}^M \mathbf{z}_{:p(k)}^{(1)} \left[\mathbf{z}_{:p(k)}^{(1)} \right]^T, & 1 \leq i \leq P \\ \sum_{k=1}^M \mathbf{z}_{:q(k)}^{(2)} \left[\mathbf{z}_{:q(k)}^{(2)} \right]^T, & P < i \leq P+Q \end{cases}$$

where $p(k) = (k-1) \times P + i$, $q(k) = (k-1) \times Q + i - P$, and \mathbf{F}_{P+Q+1} is the identity matrix with appropriate dimensions. The subscript “: i ” represents the i th column of a matrix.

Assume that \mathbf{Y} follows a multivariate normal distribution, and let n be the dimension of \mathbf{Y} . The pdf function

$$f(\mathbf{Y}) = (2\pi)^{-\frac{1}{2}n} |\boldsymbol{\Sigma}_Y|^{-\frac{1}{2}} e^{-\frac{1}{2}(\mathbf{Y}-\boldsymbol{\mu}_Y)^T \boldsymbol{\Sigma}_Y^{-1}(\mathbf{Y}-\boldsymbol{\mu}_Y)}. \quad (9)$$

This yields the log-likelihood function of \mathbf{U} and σ_j^2 , $j = 1, 2, \dots, P+Q+1$, given the observed data \mathbf{Y} and the known coefficient matrices

$$L(\mathbf{U}, \boldsymbol{\Sigma}_Y | \mathbf{Y}) = -\frac{n}{2} \ln(2\pi) - \frac{1}{2} \ln |\boldsymbol{\Sigma}_Y| - \frac{1}{2} (\mathbf{Y} - \boldsymbol{\Gamma}\mathbf{U})^T \boldsymbol{\Sigma}_Y^{-1} (\mathbf{Y} - \boldsymbol{\Gamma}\mathbf{U}). \quad (10)$$

The MLE $(\hat{\mathbf{U}})_{\text{ML}}$ and

$$(\hat{\boldsymbol{\theta}})_{\text{ML}} = [(\hat{\sigma}_1^2)_{\text{ML}} \cdots (\hat{\sigma}_{P+Q+1}^2)_{\text{ML}}]^T$$

can be obtained by numerically maximizing the log-likelihood function with respect to the mean and variance components of the process faults. The details of these optimization methods can be found in [29].

When the sample size is large, the MLE requires large computational efforts. Calculation of the MINQUE is much faster than that of the ML estimator. According to [26], the MINQEs of the variance components σ_j^2 , $j = 1, 2, \dots, P+Q+1$ are obtained by solving the MINQUE equations

$$\sum_{i=1}^{P+Q+1} [\mathbf{S}]_{ij} \hat{\sigma}_i^2 = q_j, \quad j = 1, \dots, P+Q+1 \quad (11)$$

where $[\mathbf{S}]_{ij} = \text{tr}(\mathbf{F}_i(\mathbf{M}\boldsymbol{\Sigma}_{\theta_0}\mathbf{M})^+ \mathbf{F}_j(\mathbf{M}\boldsymbol{\Sigma}_{\theta_0}\mathbf{M})^+)$, $\mathbf{M} = \mathbf{I} - \boldsymbol{\Gamma}(\boldsymbol{\Gamma}^T\boldsymbol{\Gamma})^{-1}\boldsymbol{\Gamma}^T$, $\boldsymbol{\Sigma}_{\theta_0} = \sum_{i=1}^{P+Q+1} \sigma_{\theta_0,i}^2 \mathbf{F}_i$ is an initial guess of the covariance matrix $\boldsymbol{\Sigma}_Y$ based on an *a priori* selection of variance components $\boldsymbol{\theta}_0 = [\sigma_{\theta_0,1}^2, \dots, \sigma_{\theta_0,P+Q+1}^2]^T$, $q_j = \mathbf{Y}^T(\mathbf{M}\boldsymbol{\Sigma}_{\theta_0}\mathbf{M})^+ \mathbf{F}_j(\mathbf{M}\boldsymbol{\Sigma}_{\theta_0}\mathbf{M})^+ \mathbf{Y}$, $\text{tr}(\cdot)$ is the trace of a matrix, and \mathbf{A}^+ and \mathbf{A}^- denote the Moore–Penrose inverse and a generalized inverse of a matrix \mathbf{A} , respectively. The estimate of \mathbf{U} can be obtained by using the Gauss–Markov theorem based on the MINQUE estimate of variance components denoted as $\hat{\boldsymbol{\theta}} = [\hat{\sigma}_1^2, \dots, \hat{\sigma}_{P+Q+1}^2]^T$. Let $\boldsymbol{\Sigma}_{\hat{\boldsymbol{\theta}}}$ be an estimate of $\boldsymbol{\Sigma}_Y$ given $\hat{\boldsymbol{\theta}}$, then

$$\hat{\mathbf{U}} = (\boldsymbol{\Gamma}^T \boldsymbol{\Sigma}_{\hat{\boldsymbol{\theta}}}^{-1} \boldsymbol{\Gamma})^{-1} \boldsymbol{\Gamma}^T \boldsymbol{\Sigma}_{\hat{\boldsymbol{\theta}}}^{-1} \mathbf{Y} \quad (12)$$

is a least-squares estimator of \mathbf{U} [30].

It needs to be pointed out that one critique of the ML method is the choice of a particular distribution of the measurement \mathbf{Y} . In this study, we used the most commonly used assumption: the measurement \mathbf{Y} is normally distributed. The rationale behind this assumption is that the product quality of a manufacturing process is affected by many independent random factors and disturbances. Based on the central limit theorem, the quality measurement \mathbf{Y} will tend to be normally distributed. Another issue is the robustness of the ML method. In general, the discussion of the robustness of the ML method when the model is miss-specified is very involved. Some theoretical and simulation studies indicate that the ML is fairly robust as long as the assumption is not too far from the truth, although there are no generic results on the limits of robustness [31].

For root-cause identification, only the point estimation as shown above is not sufficient to make a conclusion on the existence of process faults. A hypothesis-testing method based on estimation results needs to be developed to give the statistical significance of the faults.

III. HYPOTHESIS-TESTING METHODS FOR ROOT-CAUSE IDENTIFICATION

Process variations cannot be completely avoided for a manufacturing process. As a result, σ_i^2 , $i = 1, \dots, P$ are nonzero even in the normal condition. We assume that $\sigma_i^2 \leq h_i$, $i = 1, \dots, P$ in normal condition, where h_i is the design tolerance associated with fault i . If fault i occurs, either a nonzero mean deviation occurs on it, or its variance goes beyond the initial design tolerance. Formally, a variance change of fault i occurs if $\sigma_i^2 > h_i$; a mean shift of fault i occurs if $\mu_i \neq 0$. To identify a variance change of fault i , we study the hypothesis test for

$$H_0 : \sigma_i^2 \leq h_i \text{ versus } H_1 : \sigma_i^2 > h_i. \quad (13)$$

To identify a mean shift of fault i , we study the hypothesis test for

$$H_0 : \mu_i = 0 \text{ versus } H_1 : \mu_i \neq 0. \quad (14)$$

Reviews of literature on hypothesis tests of variance components and fixed effects in linear mixed models can be found in [32]–[34]. A majority of the literature on tests of variance components focuses

on balanced and unbalanced layout models. For most of the practical hypotheses in a balanced mixed model, optimum tests like uniformly most powerful unbiased (UMPU), uniformly most powerful invariant (UMPI), and uniformly most powerful invariant unbiased (UMPIU) do exist and coincide with the standard F tests from the associated ANOVA tables. For the unbalanced layout model, the analysis of testing significance of variance components is somewhat complicated. No exact or optimum test procedures were known for testing hypotheses in unbalanced models, except in a few special cases. Only a few of the existing hypothesis-testing procedures can be extended to the general linear mixed model. Little is known about the optimality of tests in the general linear mixed models. Seifert [35] derived an exact test for variance components and fixed effects for the general linear mixed models. However, that procedure is very complicated for models with more than two variance components. Kleffe and Seifert [36] discussed two-sided approximate testing procedures of a variance component based on MINQUE.

Stern and Welsh [37] studied the likelihood-based hypothesis tests of variance components. In this paper, we will use a likelihood-based procedure as described in [37] to test the one-sided hypothesis in (13). This procedure requires the calculation of the ML estimators, which may take infeasible computation time for systems with a large number of variance components. Therefore, a procedure using the iterated MINQUE to approximate MLE is proposed in this paper to achieve more applicable solutions.

As in [37], a common likelihood-based hypothesis testing procedure for a general linear mixed model is based on a normal-approximation to the distribution of the ML estimators. Asymptotic sampling variance of ML estimators are obtained from inverse of the information matrix $I(\mathbf{U}, \boldsymbol{\theta})$, which is defined as $I(\mathbf{U}, \boldsymbol{\theta}) = -E[\nabla^2 L(\mathbf{U}, \boldsymbol{\theta})]$. From (10), $I(\mathbf{U}, \boldsymbol{\theta})$ can be calculated as [34]

$$I(\mathbf{U}, \boldsymbol{\theta}) = \begin{bmatrix} \boldsymbol{\Gamma}^T \boldsymbol{\Sigma}_Y^{-1} \boldsymbol{\Gamma} & \mathbf{0} \\ \mathbf{0} & \frac{1}{2} \{ \text{tr}(\boldsymbol{\Sigma}_Y^{-1} \mathbf{F}_i \boldsymbol{\Sigma}_Y^{-1} \mathbf{F}_j) \}_{i,j=0}^{P+Q+1} \end{bmatrix}. \quad (15)$$

where $\{ \cdot \}_{i,j=0}^{P+Q+1}$ represents a $(P+Q+1)$ by $(P+Q+1)$ matrix. Inverting (15) gives

$$\text{var}_\infty(\hat{\mathbf{U}})_{\text{ML}} = \left(\boldsymbol{\Gamma}^T \boldsymbol{\Sigma}_Y^{-1} \boldsymbol{\Gamma} \right)^{-1} \quad (16)$$

$$\text{var}_\infty(\hat{\boldsymbol{\theta}})_{\text{ML}} = 2 \left[\left\{ \text{tr}(\boldsymbol{\Sigma}_Y^{-1} \mathbf{F}_i \boldsymbol{\Sigma}_Y^{-1} \mathbf{F}_j) \right\}_{i,j=0}^{P+Q+1} \right]^{-1} \quad (17)$$

and $\text{cov}_\infty((\hat{\mathbf{U}})_{\text{ML}}, (\hat{\boldsymbol{\theta}})_{\text{ML}}) = \mathbf{0}$, where the subscript “ ∞ ” means “asymptotically”. Based on (16) and (17), likelihood-based test statistics for μ_i and σ_i^2 can be constructed as

$$T_0(\mathbf{Y}) = \frac{\hat{\mu}_i}{\sqrt{\left[\left(\boldsymbol{\Gamma}^T \boldsymbol{\Sigma}_Y^{-1} \boldsymbol{\Gamma} \right)^{-1} \right]_{ii}}} \quad (18)$$

$$T_1(\mathbf{Y}) = \frac{(\hat{\sigma}_i^2)_{\text{ML}} - h_i}{\sqrt{2 \left[\left(\left\{ \text{tr}(\boldsymbol{\Sigma}_Y^{-1} \mathbf{F}_i \boldsymbol{\Sigma}_Y^{-1} \mathbf{F}_j) \right\}_{i,j=0}^{P+Q+1} \right)^{-1} \right]_{ii}}} \quad (19)$$

respectively, where $\boldsymbol{\Sigma}_{(\hat{\boldsymbol{\theta}})_{\text{ML}}}$ is $\boldsymbol{\Sigma}_Y$ evaluated at $(\hat{\boldsymbol{\theta}})_{\text{ML}}$, $[\mathbf{A}]_{ii}$ denote the (i, i) th element of a matrix \mathbf{A} . An approximate level α test for (13) and (14) is to reject H_0 in (13) if $T_1(\mathbf{Y}) > \Phi^{-1}(1 - \alpha)$ and reject H_0 in (14) if $|T_0(\mathbf{Y})| > \Phi^{-1}(1 - \alpha/2)$, where Φ denotes the standard normal cumulative distribution function. It is pointed out in [37] that the

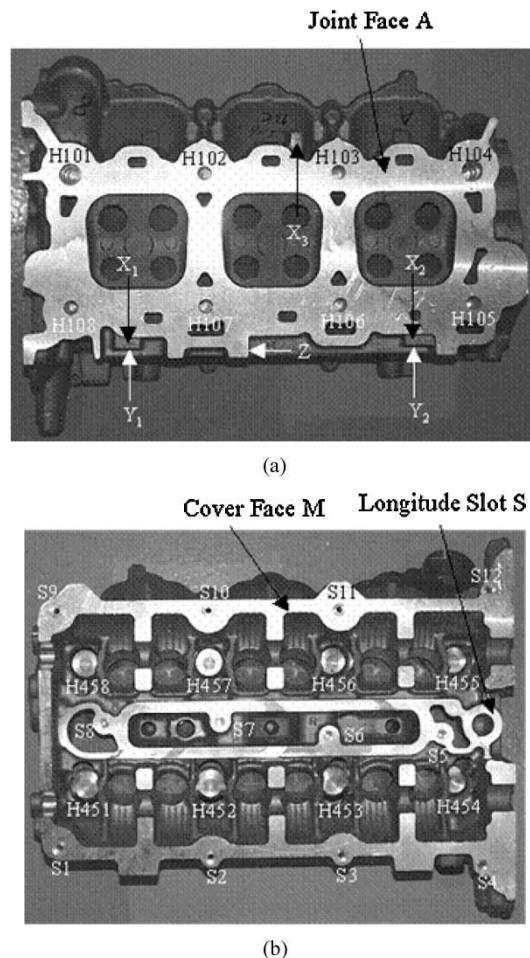


Fig. 4. Final product and its key features. (a) Joint face of the engine head. (b) Cover face of the engine head.

normal approximation used above may not be appropriate if $\boldsymbol{\theta}$ lies on the boundary of the parameter space. The parameter space of variance components is $\sigma_i \geq 0, i = 1, 2, \dots, P+Q+1$. In our model, due to the positive design tolerance associated with each fault, typically the true value of σ_i^2 cannot be zero. Therefore, the boundary problem is not significant here.

From (18) and (19), the ML estimator $(\hat{\boldsymbol{\theta}})_{\text{ML}}$ needs to be calculated to get $T_0(\mathbf{Y})$ and $T_1(\mathbf{Y})$ used in the likelihood-based hypothesis testing, which takes tremendous computation time if the number of faults in the system is large. Therefore, an alternative testing procedure based on MINQUE is proposed as follows.

Similar to the likelihood-based method, the MINQUE-based test procedure also uses the normal approximation of the estimator. Conditioning on $\boldsymbol{\theta} = \boldsymbol{\theta}_0$, the local covariance matrix of MINQUE is [38]

$$\text{var}(\hat{\boldsymbol{\theta}}) = 2\mathbf{S}^{-1} \quad (20)$$

where \mathbf{S} is defined in (11). From (12), it is easily seen that

$$\text{var}(\hat{\mathbf{U}}) = \left(\boldsymbol{\Gamma}^T \boldsymbol{\Sigma}_{\hat{\boldsymbol{\theta}}}^{-1} \boldsymbol{\Gamma} \right)^{-1} \boldsymbol{\Gamma}^T \boldsymbol{\Sigma}_{\hat{\boldsymbol{\theta}}}^{-1} \boldsymbol{\Sigma}_Y \boldsymbol{\Sigma}_{\hat{\boldsymbol{\theta}}}^{-1} \boldsymbol{\Gamma} \left[\left(\boldsymbol{\Gamma}^T \boldsymbol{\Sigma}_{\hat{\boldsymbol{\theta}}}^{-1} \boldsymbol{\Gamma} \right)^{-1} \right]^T.$$

Using $\boldsymbol{\Sigma}_{\hat{\boldsymbol{\theta}}}$, which is $\boldsymbol{\Sigma}_Y$ evaluated at $\hat{\boldsymbol{\theta}}$, to approximate $\boldsymbol{\Sigma}_Y$, the previous equation becomes

$$\text{var}(\hat{\mathbf{U}}) = \left(\boldsymbol{\Gamma}^T \boldsymbol{\Sigma}_{\hat{\boldsymbol{\theta}}}^{-1} \boldsymbol{\Gamma} \right)^{-1} \boldsymbol{\Gamma}^T \boldsymbol{\Sigma}_{\hat{\boldsymbol{\theta}}}^{-1} \boldsymbol{\Gamma} \left[\left(\boldsymbol{\Gamma}^T \boldsymbol{\Sigma}_{\hat{\boldsymbol{\theta}}}^{-1} \boldsymbol{\Gamma} \right)^{-1} \right]^T = \left(\boldsymbol{\Gamma}^T \boldsymbol{\Sigma}_{\hat{\boldsymbol{\theta}}}^{-1} \boldsymbol{\Gamma} \right)^{-1}. \quad (21)$$

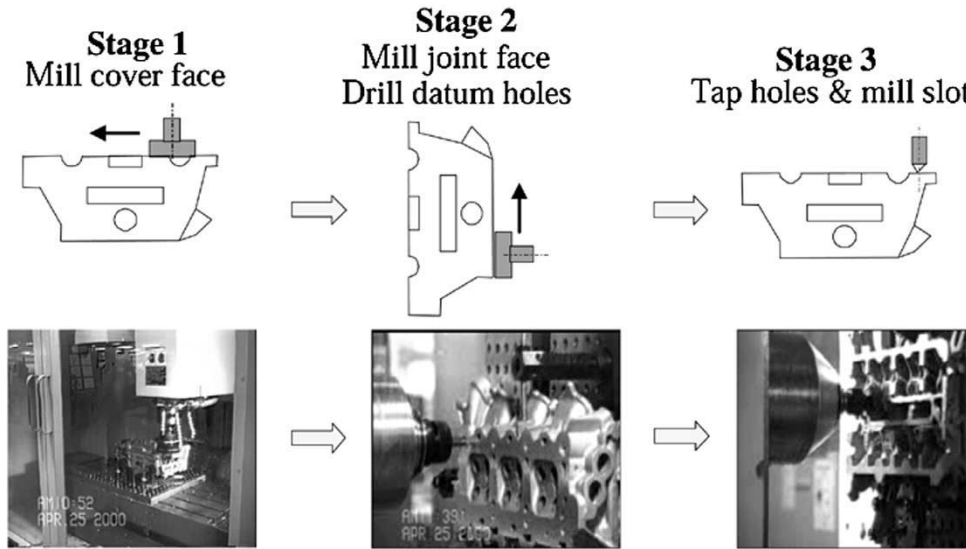


Fig. 5. Three operations.

Based on (20) and (21), MINQUE-based test statistics for μ_i and σ_i^2 can be constructed as

$$Z_0(\mathbf{Y}) = \frac{\hat{\mu}_i}{\sqrt{\left[\left(\mathbf{\Gamma}^T \mathbf{\Sigma}_{\hat{\theta}}^{-1} \mathbf{\Gamma} \right)^{-1} \right]_{ii}}} \quad (22)$$

$$Z_1(\mathbf{Y}) = \frac{\hat{\sigma}_i^2 - h_i}{\sqrt{2[\mathbf{S}^{-1}]_{ii}}} \quad (23)$$

respectively. Using normal approximation, an approximate MINQUE-based level α test for (13) and (14) is to reject H_0 in (13) if $Z_1(\mathbf{Y}) > \Phi^{-1}(1 - \alpha)$ and reject H_0 in (14) if $|Z_0(\mathbf{Y})| > \Phi^{-1}(1 - \alpha/2)$. It is clear that the asymptotic distribution of $\hat{\sigma}_i^2$ depends on the *a priori* variance components θ_0 , which can be obtained by a consistent estimator of σ_i^2 , such as MINQUE. Therefore, in this paper, we use a two-step MINQUE procedure to get $\hat{\sigma}_i^2$. The first-step MINQUE obtained by using an *a priori* value of θ is denoted by $\hat{\theta}^{(1)}$. The second-step MINQUE uses $\hat{\theta}^{(1)}$ as the *a priori* value to obtain $\hat{\sigma}_i^2$ used in (22) and (23). The asymptotic normality of the two-step MINQUE has been thoroughly discussed in [26]. In Section IV, the effectiveness of these two test procedures will be further studied through an experiment.

IV. EXPERIMENTAL STUDY

An experimental study based on a real product and production process is conducted to illustrate the root-cause identification for multistage machining processes.

A. Experimental Setup

The experiment is conducted on the hardware testbed developed at the National Science Foundation (NSF) Engineering Research Center for Reconfigurable Machining Systems. It is a three-stage machining process. The product is a V-6 automotive engine head. Its key features are shown in Fig. 4.

The key features include the cover face, joint face, datum locating holes (H101 and H104 in Fig. 4), the slot on the cover face, and extra holes on the cover and joint face (H101–H108, H451–H458, S1–S12 in Fig. 4). Besides these features, $X_1, X_2, X_3, Y_1, Y_2, Z$ are the initial locating points on the raw casting workpiece. They are used as datum for the initial cutting. The key features are machined in three stages as shown in Fig. 5.

After these machining operations, the key dimensions of the engine head are measured on a CMM. The coordinates of 15 and 16 points on the joint face and the cover face are measured to determine the dimensional integrity of these two surfaces, respectively. These measurement points are evenly distributed on these two surfaces.

Based on the process design information and the measurement scheme, a fault-quality model can be obtained (details can be found in [13]). Three features, the rough casting datum, the joint face, and the cover face, are considered in this paper. These features are only involved in the first two machining stages. Therefore, only the first and the second stages are considered in this study. From the CMM measurements of these three features after the machining operations at the second stage, we can identify certain process faults at both stage 1 and stage 2. If the system noise term is considered small and neglected to simplify the analysis, the fault-quality models for stages 1 and 2 are

$$\mathbf{Y}_i = \mathbf{\Upsilon} \mathbf{U} + \mathbf{\Upsilon} \tilde{\mathbf{U}}_i + \varepsilon_i. \quad (24)$$

$\mathbf{Y}_i \in \mathbb{R}^{31 \times 1}$ is the i th measurement sample of the cover face and the joint face. \mathbf{Y}_i includes the deviations of 15 measurement points on the cover face and 16 measurement points on the joint face. \mathbf{U} and $\tilde{\mathbf{U}}_i$ represent the locating pin position errors (mean shift and variance increase) at the 1st and the 2nd stages, respectively. \mathbf{U} and $\tilde{\mathbf{U}}_i$ are both 6 by 1 vectors. The first three elements of \mathbf{U} and $\tilde{\mathbf{U}}_i$ correspond to three pins at the first stage. The last three elements correspond to three pins at the second stage. $\mathbf{\Upsilon}$ is the coefficient matrix

$$\mathbf{\Upsilon} = \begin{bmatrix} \mathbf{\Gamma}_1 \\ \mathbf{\Gamma}_2 \end{bmatrix} \quad (25)$$

TABLE I
LOCATING PIN DEVIATION FOR EACH WORKPIECE AT ABNORMAL CONDITION (UNIT: 0.0254 mm)

Part #	1	2	3	4	5	6	7	8	9	10	11	12	13	14	15	16	17	18	19	20
d_3	10	13	12	6	7	9	8	10	7	11	5	10	9	9	9	17	15	10	11	6
d_4	9	7	8	7	7	7	5	8	12	9	4	9	11	9	9	6	8	7	5	8
d_5	1	1	1	1	1	1	1	1	1	1	1	1	1	1	1	1	1	1	1	1

where $\mathbf{\Gamma}_1 = [\mathbf{\Gamma}_{11} \ \mathbf{0}]$, $\mathbf{\Gamma}_2 = [\mathbf{0} \ \mathbf{\Gamma}_{22}]$, and

$$\mathbf{\Gamma}_{11} = \begin{bmatrix} -0.5402 & 0.9690 & 0.5711 \\ -0.6455 & 0.5991 & 1.0464 \\ -0.2664 & 0.2203 & 1.0461 \\ 0.0683 & -0.1140 & 1.0458 \\ 0.5158 & -0.5612 & 1.0453 \\ 0.8555 & -0.9005 & 1.0450 \\ 0.9902 & -0.7058 & 0.7156 \\ 1.1863 & -0.4225 & 0.2362 \\ 1.3106 & -0.2428 & -0.0678 \\ 1.0177 & 0.1052 & -0.1229 \\ 0.6394 & 0.4597 & -0.0991 \\ 0.3403 & 0.7585 & -0.0988 \\ 0.0530 & 1.0455 & -0.0985 \\ -0.0820 & 0.8192 & 0.2628 \\ -0.2776 & 0.5367 & 0.7409 \end{bmatrix}$$

$$\mathbf{\Gamma}_{22} = \begin{bmatrix} -0.6349 & 0.9602 & 0.6747 \\ -0.4590 & 0.6817 & 0.7773 \\ -0.0332 & 0.2556 & 0.7776 \\ 0.2510 & -0.0288 & 0.7778 \\ 0.6955 & -0.4736 & 0.7781 \\ 1.0215 & -0.5857 & 0.5641 \\ 1.1372 & -0.5031 & 0.3659 \\ 1.1155 & -0.3477 & 0.2322 \\ 0.9048 & -0.1368 & 0.2320 \\ 0.6472 & 0.1210 & 0.2318 \\ 0.5864 & -0.0142 & 0.4279 \\ 0.3875 & 0.3998 & 0.2127 \\ 0.0777 & 0.7098 & 0.2124 \\ -0.1490 & 0.9368 & 0.2123 \\ -0.4063 & 0.9339 & 0.4725 \\ 0.0776 & 0.4496 & 0.4728 \end{bmatrix}$$

Some readers might notice that the coefficient matrix in (25) is in a block diagonal form. It should be pointed out that this is not always true in general case. It could have any structure and even be singular. A diagnosability study is usually needed to determine if the process faults can be identified based on the quality measurements [17]. In this experimental study, the coefficient matrix is well-conditioned and the system is fully diagnosable, which means that the means and the variances of all process faults can be estimated based on the CMM measurements.

To validate the root-cause identification method developed in previous sections, eight workpieces are machined under normal condition and twenty workpieces are machined under abnormal condition. No variational errors exist in normal condition. However, due to the initial calibration, there are possible mean deviations. Under this condition, the product dimensional quality variation is caused by the natural variation of the process ("common causes" in the SPC terminology). In the abnormal condition, fixture errors are intentionally injected in the process by adding a series of shims with different thicknesses on three locating pins at the first and second stages, respectively. These three pins correspond to the third, fourth, and fifth elements of \mathbf{U} in (24).

TABLE II
ML ESTIMATION RESULTS

Pin #	$(\hat{\mu}_i)_{ML}$	$(\hat{\sigma}_i^2)_{ML}$	$T_0(\mathbf{Y})$	$T_1(\mathbf{Y})$	$(\hat{\mu}_i^*)_{ML}$	$(\hat{\sigma}_i^{*2})_{ML}$	$T_0^*(\mathbf{Y})$	$T_1^*(\mathbf{Y})$	W
1	1.2	24.4	0.57	-32.88	-2.1	139	-0.80	-10.67	-0.98
2	4.8	338.2	0.74	-1.69	0.8	193	0.27	-6.84	-0.55
3	110.6	1112.3	9.37	0.88	-196.6	7743	-9.99	2.91	-13.39
4	25.6	97.2	7.23	-10.55	-215.4	2791	-18.20	2.45	-19.51
5	-142	67.4	-47.53	-15.66	-186.8	97	-79.33	-15.12	-11.77
6	-8.9	35.6	-4.00	-30.06	-23.6	133	-8.73	-10.70	-4.21

The thicknesses of these shims are listed in Table I. They can be considered as the deviations of the position of the locating pin. For example, when the first workpiece is machined, three shims with thickness 0.254, 0.229, and 0.0254 mm are intentionally put on the third locating pin on the first stage, and the first two pins on the second stage. Besides the intentionally generated locating pin error, the cutting on the second stage in the abnormal condition is conducted when the machine is in hot condition. The purpose is to check the influence of thermal error.

The deviations of d_3 and d_4 are selected such that they approximately follow normal distribution, where $d_3 \sim N(0.25, 0.085^2)$, $d_4 \sim N(0.2, 0.06^2)$. d_5 is just a constant of 0.0254 mm. Totally, 20 workpieces are machined in this experiment and measured on a CMM. The measurement data are the deviation of the measurement points from their nominal values. The measurement data for both normal and abnormal conditions are all listed in the Appendix (Tables VI–IX).

B. Likelihood-Based Root-Cause Identification

Based on the CMM measurements, root-cause identification for this multistage engine head machining process is performed using the hypothesis testing procedures discussed in Section III. First, the MLE and the likelihood-based testing procedure are used. The results are listed in Table II.

The columns of $(\hat{\mu}_i)_{ML}$, $(\hat{\sigma}_i^2)_{ML}$, $(\hat{\mu}_i^*)_{ML}$, and $(\hat{\sigma}_i^{*2})_{ML}$ are the estimation results of the mean and variance of the deviations of the six locating pins (1–3 are at the first stage and 4–6 are at the second stage) under the normal and abnormal working conditions, respectively. The unit of $(\hat{\mu}_i)_{ML}$ and $(\hat{\mu}_i^*)_{ML}$ is 10^{-3} mm, and the unit of $(\hat{\sigma}_i^2)_{ML}$ and $(\hat{\sigma}_i^{*2})_{ML}$ is 10^{-6} mm². The design tolerance h_i is set to be $0.025^2 = 625 \times 10^{-6}$ mm², $i = 1, \dots, 6$. From (15), (18), and (19), the likelihood-based test statistics for each of the six pins under both the normal and abnormal working conditions are given by the columns of $T_0(\mathbf{Y})$, $T_1(\mathbf{Y})$, $T_0^*(\mathbf{Y})$, and $T_1^*(\mathbf{Y})$, respectively.

Select $\alpha = 0.1$. H_0 in (13) is rejected if $T_1(\mathbf{Y}) > \Phi^{-1}(1 - \alpha) = 1.28$ and H_0 in (14) is rejected if $|T_0(\mathbf{Y})| > \Phi^{-1}(1 - \alpha/2) = 1.65$. From Table II, it is concluded that, under normal working conditions, there is no variance change at any locating pins. However, there are mean deviations at pins 3–6. As explained in Section IV-A, the mean deviations of the locations of these four pins under normal condition are due to the initial calibration errors of the machining system. On the other hand, under abnormal conditions, it is concluded that there are variance changes at pin 3 and pin 4 and the mean deviations at pin 3–6. The variance testing results are consistent with the experiment very well since we intentionally injected variation errors on pins 3 and 4 during the experiment.

Since the testing results show that mean deviations exist at pins 3–6 under both normal and abnormal conditions, it is of interest to test

TABLE III
TWO-STEP MINQUE ESTIMATION RESULTS

Pin #	$\hat{\mu}_i$	$\hat{\sigma}_i^2$	$Z_0(\mathbf{Y})$	$Z_1(\mathbf{Y})$	$\hat{\mu}_i^*$	$\hat{\sigma}_i^{*2}$	$Z_0^*(\mathbf{Y})$	$Z_1^*(\mathbf{Y})$	W
1	1.2	39.6	0.53	-26.7	-2.1	147	-0.79	-9.73	-0.94
2	4.8	386.8	0.69	-1.15	0.9	203	0.26	-6.18	-0.51
3	110.6	1271.4	8.77	0.95	-196.6	8151	-9.73	2.84	-12.90
4	25.6	111.1	6.77	-8.44	-215.4	2936	-17.75	2.42	-18.96
5	-142	77.6	-44.48	-12.58	-186.8	104	-77.06	-13.72	-11.17
6	-8.9	41.2	-3.74	-4.25	-23.6	140	-8.53	-9.82	-4.04

TABLE IV
 $Z_1(\mathbf{Y})$ FOR TESTING OF σ_3^2 BASED ON DIFFERENT COMBINATIONS OF $\sigma_{0,3}^2$ AND $\sigma_{0,7}^2$

		$\sigma_{0,3}^2$ (mm ²)				
		0.0001	0.001	0.01	1	10
$\sigma_{0,7}^2$ (mm ²)	0.0001	2.844365	2.844366	2.844366	2.844366	2.844366
	0.001	2.844361	2.844366	2.844367	2.844367	2.844367
	0.01	2.844358	2.844372	2.844382	2.844384	2.844384
	1	2.844337	2.844337	2.844342	2.844378	2.844380
	10	2.844337	2.844337	2.844337	2.844362	2.844378

TABLE V
SAMPLE MEAN AND STANDARD DEVIATION OF $Z_0(\mathbf{Y})$ AND $Z_1(\mathbf{Y})$

i	1	2	3	4	5	6
$\bar{Z}_0(\mathbf{Y})$	0.0035	-0.0087	-0.0095	0.0068	-0.0171	-0.0284
$S_{Z_0(\mathbf{Y})}$	1.0681	1.0053	1.0767	1.0437	1.0540	1.0741
$\bar{Z}_1(\mathbf{Y})$	-0.3457	-0.3767	-0.3558	-0.3934	-0.3633	-0.3436
$S_{Z_1(\mathbf{Y})}$	1.1967	1.2201	1.1882	1.3098	1.2248	1.2303

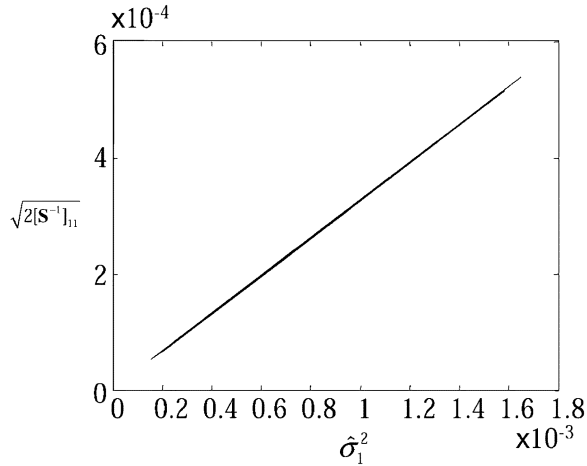


Fig. 6. Relation between $\sqrt{2[\mathbf{S}^{-1}]_{11}}$ and $\hat{\sigma}_1^2$.

whether there is a significant mean shift on these pins from the normal condition to the abnormal condition. Let $\hat{\mu}_{i0}$ denote the estimation of μ_i in normal condition; and $\hat{\mu}_{i1}$ the estimation of μ_i in abnormal condition. Since $\hat{\mu}_{i0}$ and $\hat{\mu}_{i1}$ are independent and both approximately normally distributed, $\hat{\mu}_{i0} - \hat{\mu}_{i1}$ approximately follows normal distribution with mean $\mu_{i0} - \mu_{i1}$ and variance $\text{var}(\hat{\mu}_{i0}) + \text{var}(\hat{\mu}_{i1})$. Therefore, a test statistic can be constructed as

$$W(\mathbf{Y}) = \frac{\hat{\mu}_{i0} - \hat{\mu}_{i1}}{\sqrt{\text{var}(\hat{\mu}_{i0}) + \text{var}(\hat{\mu}_{i1})}} \quad (26)$$

where $\text{var}(\hat{\mu}_{i0})$ and $\text{var}(\hat{\mu}_{i1})$ are calculated by (16) for the MLE or (21) for the MINQUE. Identification of mean shifts between different

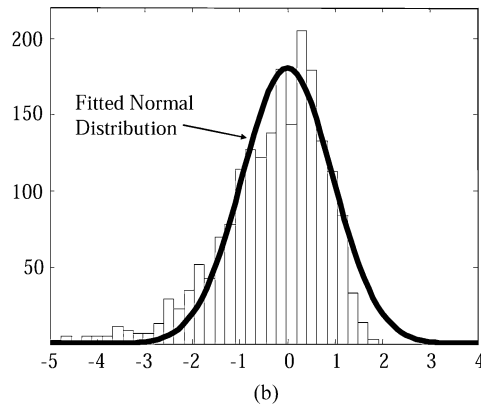
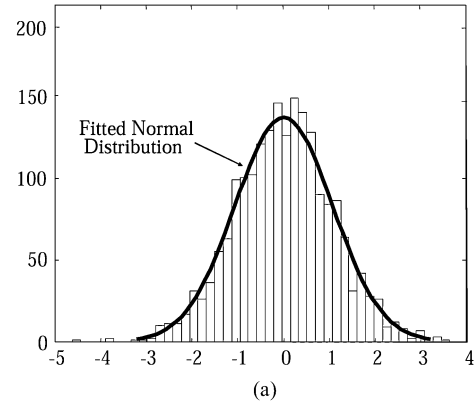


Fig. 7. (a) Histogram of $Z_0(\mathbf{Y})$. (b) Histogram of $Z_1(\mathbf{Y})$.

working conditions can be formulated as the following hypothesis testing problem:

$$H_0 : \mu_{i0} = \mu_{i1} \text{ versus } H_1 : \mu_{i0} \neq \mu_{i1} \quad (27)$$

TABLE VI
COVER FACE MEASUREMENTS UNDER *NORMAL* CONDITION (UNIT: MILLIMETERS)

Part #	1	2	3	4	5	6	7	8	9	10	11	12	13	14	15
1	0.1065	0.1945	0.1772	0.1681	0.1749	0.175	0.1238	0.0422	-0.0117	-0.021	-0.0193	-0.0184	-0.0157	0.0511	0.1287
2	0.0603	0.1111	0.1019	0.0992	0.1089	0.1154	0.0899	0.0411	0.0105	0.0017	-0.005	-0.0092	-0.0116	0.0293	0.0744
3	0.0615	0.1175	0.1047	0.0998	0.1098	0.113	0.0821	0.0286	-0.0042	-0.0124	-0.015	-0.0175	-0.0176	0.0267	0.0754
4	0.0964	0.1576	0.1476	0.1486	0.1684	0.1757	0.1266	0.0512	0.0004	-0.0122	-0.0154	-0.0193	-0.0227	0.0368	0.1014
5	0.0441	0.0777	0.067	0.0644	0.071	0.0697	0.0543	0.0221	-0.0006	-0.0032	-0.0046	-0.0064	-0.0065	0.0236	0.0517
6	0.0525	0.0924	0.0793	0.073	0.0802	0.0805	0.0592	0.0199	-0.0044	-0.0093	-0.01	-0.0104	-0.0083	0.0262	0.0593
7	0.1044	0.1328	0.1002	0.079	0.0597	0.0448	0.031	0.0009	-0.0204	-0.0062	0.0101	0.0246	0.0429	0.0677	0.0958
8	0.0613	0.1233	0.1121	0.1106	0.1252	0.1316	0.0902	0.025	-0.0188	-0.0273	-0.0267	-0.0273	-0.026	0.0243	0.0768

TABLE VII
JOINT FACE MEASUREMENTS UNDER *NORMAL* CONDITION (UNIT: MILLIMETERS)

Part #	1	2	3	4	5	6	7	8	9	10	11	12	13	14	15	16
1	-0.1637	-0.1277	-0.0572	-0.0054	0.0705	0.1	0.0941	0.0718	0.0379	-0.0072	0.0082	-0.0514	-0.1013	-0.1346	-0.1568	-0.0774
2	-0.1551	-0.1176	-0.0479	0.0015	0.0751	0.1035	0.0977	0.075	0.0421	-0.0016	0.0129	-0.0466	-0.0989	-0.1321	-0.1505	-0.0699
3	-0.1581	-0.119	-0.0417	0.0136	0.0949	0.1225	0.1115	0.0851	0.0477	0.0033	0.0209	-0.0434	-0.1024	-0.136	-0.1536	-0.066
4	-0.1593	-0.1224	-0.0434	0.0078	0.0916	0.1251	0.1178	0.0907	0.052	0.0022	0.022	-0.0462	-0.0998	-0.1359	-0.1576	-0.0704
5	-0.167	-0.1237	-0.0524	0.0039	0.0871	0.1151	0.1052	0.0789	0.0414	-0.0051	0.0115	-0.0503	-0.1085	-0.1447	-0.1624	-0.0773
6	-0.1297	-0.0999	-0.044	-0.0026	0.0594	0.0784	0.07	0.0482	0.0184	-0.0162	0.0006	-0.0507	-0.0937	-0.1196	-0.1321	-0.067
7	-0.1411	-0.1093	-0.0417	0.01	0.0793	0.1086	0.1019	0.0787	0.0454	-0.0002	0.0149	-0.0409	-0.0953	-0.1199	-0.1411	-0.0656
8	-0.1544	-0.1182	-0.0492	0.0046	0.0808	0.1073	0.0926	0.065	0.0316	-0.0144	0.0069	-0.0571	-0.109	-0.1383	-0.1531	-0.0747

where H_0 is rejected if $|W| > \Phi^{-1}(1 - \alpha/2)$. The test statistic W using the MLE is calculated for each pin and listed in the last column of Table II.

Comparing $|W|$ based on Table II with $\Phi^{-1}(1 - \alpha/2) = \Phi^{-1}(0.95) = 1.65$. Faults 3, 4, 5, and 6 all have negative mean shifts, which means that the positions of the locating pins have upward shifts from normal condition to abnormal condition. The mean shift of pin 3 is due to the shims on pin 3. The mean shifts on pin 4, 5, and 6 are due to both the inserted shims and the thermal error. Thermal error is manifested as an increase in the length of the spindle, which is equivalent to an upward error in all the location pins in the fixture. Therefore, not only pins 4 and 5 are identified to have a mean shift, but pin 6 is also identified to have a mean shift. This hints that if two types of machine errors have the same manifestation on the product quality, we will not be able to distinguish them.

C. MINQUE-Based Root-Cause Identification

MLE is a very powerful tool for root-cause identification. However, the computational load for MLE is high in general. The MINQUE-based testing procedure is proposed to save computational time. It is a natural choice to select the *a priori* value of the variance components as the design tolerance h_i at the first-step MINQUE. The estimation results of the two-step MINQUE are listed in Table III.

Select $\alpha = 0.1$, H_0 in (13) is rejected if $Z_1(\mathbf{Y}) > \Phi^{-1}(1 - \alpha) = 1.28$ and H_0 in (14) is rejected if $|Z_0(\mathbf{Y})| > \Phi^{-1}(1 - \alpha/2) = 1.65$. From Table III, it is concluded that there is no variance change at any pin locations and the mean deviations exist on pins 3–6 under the normal working condition. On the other hand, under abnormal working condition, it can be concluded that there are variance changes at pins 3 and 4 and mean deviations at pins 3–6. This result is consistent with the conclusion of the likelihood-based testing results.

The test on the mean shifts between the normal condition and abnormal condition can also be based on the MINQUE procedure. The test statistics of (26) for the test in (27) based on MINQUE are listed in the last column of Table III.

Comparing $|W|$ based on Table III with $\Phi^{-1}(1 - \alpha/2) = \Phi^{-1}(0.95) = 1.65$, the testing results are consistent with the results based on the MLE.

Comparing the MINQUE and MLE in this example, they are fairly close. The estimation of the mean value is almost the same to each other. There are some discrepancies in the estimation of the variance components. However, the discrepancy of the two estimation methods does not have essential impact on the hypothesis testing results in this experimental study. Therefore, for the machining processes as used in this case study, the MINQUE-based procedure is a good alternative to the likelihood-based procedure.

D. Discussion on MINQUE-Based Procedure

1) *Robustness of MINQUE-Based Procedure to the Selection of a Priori Variance Components*: It is clear that the MINQUE-based testing results depend on the selection of θ_0 , the *a priori* value of the first-step MINQUE. Table IV lists the MINQUE-based test statistic $Z_1(\mathbf{Y})$ for the variance component σ_3^2 based on the data from abnormal condition. Different combinations of the *a priori* values for the variance of deviation of pin 3 ($\sigma_{0,3}^2$) and the measurement error variance ($\sigma_{0,7}^2$) are used in Table IV, while the other *a priori* values are fixed as the design tolerance h_i . Similar tables can be generated for other pins. From this table, it is obvious that the two-step MINQUE is pretty robust to the selection of the *a priori* value of the parameters.

2) *Normality of the Test Statistics*: In this paper, we use normal distribution as the approximate distribution of the test statistics. The normality is only true asymptotically. Under moderate samples (sample size 20 in this paper), the distribution is different from normal. In this section, the distribution of the test statistics under a sample size of 20 is investigated based on simulation. The deviation of locating pin i is randomly generated following $N(0, h_i)$, where h_i is the design tolerance which is 0.025^2 mm^2 for all the pins. The measurement errors are randomly generated following $N(0, 0.01^2)$. Therefore, the observation vector \mathbf{Y} can be calculated based on (6). For each simulation, \mathbf{Y} corresponding to 20 parts are generated and

TABLE VIII
COVER FACE MEASUREMENTS UNDER *ABNORMAL* CONDITION (UNIT: MILLIMETERS)

Part #	1	2	3	4	5	6	7	8	9	10	11	12	13	14	15
1	-0.093	-0.1974	-0.2159	-0.227	-0.233	-0.2404	-0.1642	-0.0591	0.0039	0.025	0.0238	0.0305	0.038	-0.0339	-0.144
2	-0.104	-0.22	-0.2459	-0.2619	-0.275	-0.2887	-0.1999	-0.0824	-0.0127	0.0149	0.019	0.0323	0.0441	-0.0391	-0.1617
3	-0.0852	-0.173	-0.1962	-0.2071	-0.2136	-0.2164	-0.1512	-0.0593	-0.0085	0.0107	0.0112	0.0194	0.0262	-0.0353	-0.1313
4	-0.0951	-0.1879	-0.1975	-0.1988	-0.1917	-0.1909	-0.1181	-0.0229	0.0352	0.0451	0.0356	0.0337	0.0308	-0.0336	-0.1336
5	-0.1263	-0.2417	-0.2536	-0.2541	-0.2441	-0.2432	-0.1558	-0.0391	0.0319	0.0445	0.0337	0.0329	0.0295	-0.0499	-0.1713
6	-0.1302	-0.24	-0.2575	-0.2606	-0.2594	-0.2602	-0.1821	-0.0748	-0.0086	0.0063	0.0027	0.008	0.0145	-0.0638	-0.1792
7	-0.1621	-0.2916	-0.3091	-0.3121	-0.3135	-0.3141	-0.2237	-0.0902	-0.0134	0.0054	-0.0005	0.0043	0.0082	-0.0844	-0.2186
8	-0.1872	-0.3385	-0.3499	-0.3498	-0.3371	-0.3312	-0.2244	-0.069	0.0235	0.0381	0.0255	0.0237	0.0208	-0.0893	-0.2465
9	-0.195	-0.3488	-0.3578	-0.3537	-0.3397	-0.3355	-0.2254	-0.073	0.0224	0.0383	0.0245	0.0237	0.0222	-0.0904	-0.2527
10	-0.1894	-0.3913	-0.4197	-0.4351	-0.4456	-0.4603	-0.319	-0.1158	0.0062	0.0429	0.0441	0.0596	0.0735	-0.0739	-0.2789
11	-0.1021	-0.1851	-0.198	-0.1994	-0.1901	-0.1859	-0.1237	-0.038	0.0153	0.0228	0.0135	0.0113	0.0099	-0.0481	-0.1407
12	-0.0943	-0.1698	-0.1773	-0.1738	-0.1601	-0.1517	-0.0974	-0.0229	0.0226	0.026	0.0145	0.0105	0.0067	-0.0445	-0.1254
13	-0.0873	-0.1758	-0.1902	-0.1941	-0.1874	-0.1853	-0.1212	-0.0325	0.0196	0.0307	0.0273	0.0281	0.0296	-0.0291	-0.1199
14	-0.0896	-0.1685	-0.176	-0.1735	-0.1597	-0.155	-0.0965	-0.0195	0.0255	0.0322	0.0234	0.0201	0.0171	-0.0374	-0.1221
15	-0.0309	-0.0681	-0.0761	-0.076	-0.0653	-0.0616	-0.0357	-0.0029	0.0141	0.0158	0.0091	0.0061	0.0046	-0.0153	-0.0512
16	-0.0602	-0.1007	-0.1135	-0.1165	-0.1072	-0.1047	-0.0687	-0.0235	0.0029	0.0059	-0.0023	-0.0055	-0.0065	-0.0347	-0.0841
17	-0.067	-0.1109	-0.1211	-0.1222	-0.1116	-0.1064	-0.0707	-0.0246	0.002	0.0027	-0.007	-0.0105	-0.0137	-0.0415	-0.0901
18	-0.0584	-0.0985	-0.1135	-0.1161	-0.1071	-0.1056	-0.0678	-0.022	0.0001	0.004	-0.0038	-0.0035	-0.0035	-0.0313	-0.078
19	-0.0518	-0.0879	-0.0985	-0.0972	-0.0834	-0.0792	-0.0523	-0.0108	0.0109	0.0101	0.0014	-0.0008	-0.0016	-0.0276	-0.0703
20	-0.0855	-0.1459	-0.1545	-0.1518	-0.1357	-0.1312	-0.0831	-0.0188	0.0169	0.0182	0.0079	0.0043	0.0021	-0.0427	-0.1117

TABLE IX
JOINT FACE MEASUREMENTS UNDER *ABNORMAL* CONDITION (UNIT: mm)

#	1	2	3	4	5	6	7	8	9	10	11	12	13	14	15	16
1	-0.0668	-0.0602	-0.0672	-0.0673	-0.074	-0.1132	-0.1363	-0.161	-0.162	-0.1583	-0.122	-0.1589	-0.1556	-0.1498	-0.1191	-0.12
2	-0.0868	-0.0731	-0.0598	-0.0442	-0.0286	-0.0509	-0.0773	-0.101	-0.1069	-0.1158	-0.0911	-0.1294	-0.1383	-0.1428	-0.1261	-0.1026
3	-0.1101	-0.0908	-0.0618	-0.0366	-0.007	-0.0191	-0.0379	-0.0666	-0.0829	-0.1024	-0.0722	-0.1219	-0.1463	-0.1552	-0.1401	-0.1049
4	-0.0957	-0.0768	-0.0612	-0.0441	-0.0245	-0.0523	-0.0808	-0.1138	-0.1255	-0.1327	-0.0987	-0.1449	-0.1572	-0.1591	-0.1321	-0.1143
5	-0.0743	-0.0606	-0.0545	-0.0419	-0.0345	-0.0698	-0.1072	-0.1412	-0.1473	-0.15	-0.1094	-0.1564	-0.1597	-0.1556	-0.1188	-0.1103
6	-0.0703	-0.0662	-0.0754	-0.0711	-0.0812	-0.1164	-0.1416	-0.1665	-0.1663	-0.1634	-0.134	-0.1599	-0.1591	-0.147	-0.1154	-0.1242
7	-0.0753	-0.0683	-0.0746	-0.0684	-0.0724	-0.1038	-0.1287	-0.1517	-0.15	-0.1526	-0.1257	-0.1529	-0.1527	-0.1419	-0.1151	-0.119
8	-0.0559	-0.0531	-0.0671	-0.0657	-0.0791	-0.1179	-0.1447	-0.1657	-0.164	-0.1591	-0.1273	-0.1529	-0.1478	-0.1341	-0.1006	-0.1117
9	-0.0643	-0.0583	-0.0683	-0.0647	-0.0736	-0.1089	-0.1382	-0.1635	-0.16	-0.1583	-0.128	-0.1546	-0.1516	-0.1389	-0.1034	-0.116
10	-0.0603	-0.0556	-0.0666	-0.0655	-0.0748	-0.1123	-0.1419	-0.1686	-0.1619	-0.1601	-0.1286	-0.1559	-0.1509	-0.1385	-0.1038	-0.1137
11	-0.0598	-0.0572	-0.0755	-0.0775	-0.0957	-0.1405	-0.1717	-0.1994	-0.1947	-0.1863	-0.1519	-0.1787	-0.1697	-0.1512	-0.1112	-0.13
12	-0.0437	-0.0423	-0.0603	-0.0619	-0.0803	-0.1254	-0.1588	-0.1856	-0.1806	-0.1735	-0.1354	-0.1653	-0.1562	-0.1407	-0.101	-0.1167
13	-0.033	-0.0362	-0.0533	-0.054	-0.0685	-0.1091	-0.1373	-0.1627	-0.156	-0.1546	-0.1197	-0.1486	-0.1417	-0.1296	-0.0935	-0.1063
14	-0.0392	-0.0369	-0.0619	-0.07	-0.0931	-0.1509	-0.1888	-0.2183	-0.2085	-0.1955	-0.1558	-0.1822	-0.1672	-0.1467	-0.0972	-0.124
15	-0.0548	-0.043	-0.0559	-0.0501	-0.0529	-0.107	-0.1417	-0.1744	-0.1727	-0.1712	-0.1305	-0.1699	-0.1652	-0.1546	-0.1116	-0.1204
16	-0.0258	-0.0322	-0.0679	-0.0811	-0.1168	-0.1686	-0.2033	-0.2272	-0.2084	-0.1932	-0.1603	-0.1738	-0.1512	-0.1248	-0.0782	-0.1178
17	-0.0316	-0.0327	-0.0647	-0.0762	-0.1084	-0.1643	-0.1986	-0.2257	-0.2121	-0.1921	-0.1567	-0.1756	-0.1568	-0.1303	-0.0819	-0.1175
18	-0.0128	-0.0146	-0.0409	-0.0473	-0.0747	-0.1336	-0.1756	-0.2079	-0.1952	-0.1817	-0.1434	-0.1678	-0.1517	-0.1253	-0.0771	-0.11
19	0.0035	-0.0124	-0.0724	-0.1023	-0.1634	-0.234	-0.275	-0.2972	-0.2676	-0.2364	-0.1979	-0.2033	-0.1618	-0.1234	-0.0606	-0.1292
20	0.021	0.0053	-0.0634	-0.0984	-0.1696	-0.2593	-0.3079	-0.332	-0.3038	-0.2602	-0.2144	-0.2203	-0.1722	-0.1301	-0.054	-0.1311

the MINQUE-based testing procedure is used based on \mathbf{Y} to get the test statistics $Z_0(\mathbf{Y})$ and $Z_1(\mathbf{Y})$. Totally, 2000 such simulations are used to estimate the distribution of $Z_0(\mathbf{Y})$ and $Z_1(\mathbf{Y})$. The sample means and standard deviations of $Z_0(\mathbf{Y})$ and $Z_1(\mathbf{Y})$ for each pin are listed in Table V.

From Table V, the sample mean and standard deviation of $Z_0(\mathbf{Y})$ is fairly close to 0 and 1, respectively, while those of $Z_1(\mathbf{Y})$ are biased. All the sample variances of both $Z_0(\mathbf{Y})$ and $Z_1(\mathbf{Y})$ are greater than one. This is reasonable because generally the variance of the estimator increases with the decrease of the sample size. Therefore, the variance of the test statistic with finite sample size is larger than that of the test statistic with an infinite large sample size. The variance of the test statistic with sample size going to infinite is the asymptotic variance, which is one. $Z_1(\mathbf{Y})$ has larger bias from the asymptotic distribution than $Z_0(\mathbf{Y})$ because the accuracy of the variance components estimation in a linear mixed model with small sample size is worse than

that of the estimation of fixed effect. This is also why the MINQUE and MLE have larger discrepancy for the pin height variance estimation than for the pin height mean estimation.

Since $\hat{\sigma}_i^2$ is an unbiased estimator, the sample average of $\hat{\sigma}_i^2 - h_i$ should be close to zero. But why does $\bar{Z}_1(\mathbf{Y})$ have uniformly negative mean values in Table V? It can be explained by Fig. 6.

Fig. 6 plots $\sqrt{2[\mathbf{S}^{-1}]_{11}}$, which is the denominator of $Z_1(\mathbf{Y})$ in (23) for testing variance of pin 1, versus $\hat{\sigma}_1^2$, the MINQUE of pin 1. It can be seen clearly from Fig. 6 that smaller estimation of the variance component leads to smaller $\sqrt{2[\mathbf{S}^{-1}]_{11}}$, and the average of $Z_1(\mathbf{Y})$ can be considered as a weighted average of $\hat{\sigma}_1^2 - h_1$, the numerator of (23), with the weights larger for smaller $\hat{\sigma}_1^2 - h_1$. As a result, even if the average of $\hat{\sigma}_1^2 - h_1$ is close to zero, the average of $Z_1(\mathbf{Y})$ is smaller than zero.

We have examined the first two moments of the distribution of the test statistics. Now, let us look at the shape of the distribution and com-

pare it with that of the normal distribution. Fig. 7 shows the histogram of $Z_0(\mathbf{Y})$ and $Z_1(\mathbf{Y})$ for pin 1 fitted with normal density.

It can be seen that the shape of the distribution of $Z_0(\mathbf{Y})$ is very close to that of the normal density. The distribution of $Z_1(\mathbf{Y})$ is in fact a little skewed. Quantiles of the simulated test statistics distribution are compared with that of the standard normal distribution. The true α quantile of the simulated distribution of the test statistic can be simply estimated by the $(2000 \times \alpha)$ th order statistic of the test statistics calculated from the 2000 simulations. For $Z_0(\mathbf{Y})$ of pin 1, the estimated 5% and 95% quantiles based on the simulations are -1.78 and 1.76 , respectively. For $Z_1(\mathbf{Y})$ of pin 1, the estimated 90% quantile is 1.14 . Compared with the 5% and 95% quantiles of standard normal distribution, which are -1.65 and 1.65 , and 90% quantile of standard normal distribution, which is 1.28 , the quantiles of the simulated distribution of $Z_0(\mathbf{Y})$ and $Z_1(\mathbf{Y})$ are close to those of the standard normal distribution.

Based on above discussion, the testing procedure using normal distribution as approximated distribution can achieve satisfactory probability.

V. CONCLUDING REMARKS

In this paper, a methodology for root-cause identification of multistage manufacturing processes is developed. The root-cause identification is formulated as a problem of fixed and random effect estimation and hypothesis testing for a general linear mixed model. The experimental study shows that the variance components estimation and the proposed testing procedure is an effective technique for the challenging engineering problem of root-cause identification for multistage manufacturing processes.

It should be pointed out that the model used in this study is derived from the physics of the process. Under other circumstances where the inter-relationship among those characteristics is unknown, this model can also be obtained through statistical or other model fitting methods. In either case, the effect of the model uncertainty should be considered in the estimation and the hypothesis testing procedure, which is our future research.

APPENDIX

The experiment measurement data are given in (Tables VI–IX).

ACKNOWLEDGMENT

The authors would like to thank the editor and referees for their valuable comments and suggestions.

REFERENCES

- [1] D. C. Montgomery and W. H. Woodall, "A discussion on statistically-based process monitoring and control," *J. Qual. Technol.*, vol. 29, pp. 121–162, 1997.
- [2] W. H. Woodall and D. C. Montgomery, "Research issues and ideas in statistical process control," *J. Qual. Technol.*, vol. 31, pp. 376–386, 1999.
- [3] D. Ceglarek and J. Shi, "Dimensional variation reduction for automotive body assembly," *J. Manufact. Rev.*, vol. 8, pp. 139–154, 1995.
- [4] J. C. Quinlan. (1998, Oct.) On-machine probing key to parts quality. *Qual. Manufact.* [Online]. Available: <http://www.manufacturing-center.com/qm/archives/1098/1098mp.as>
- [5] D. Ceglarek and J. Shi, "Fixture failure diagnosis for autobody assembly using pattern recognition," *ASME J. Eng. Ind.*, vol. 188, pp. 55–65, 1996.
- [6] Q. Rong, D. Ceglarek, and J. Shi, "Dimensional fault diagnosis for compliant beam structure assemblies," *ASME J. Manufact. Sci. Eng.*, vol. 122, pp. 773–780, 2000.
- [7] M. Chang and D. C. Gossard, "Computational method for diagnosis of variation-related assembly problem," *Int. J. Prod. Res.*, vol. 36, pp. 2985–2995, 1998.

- [8] D. W. Apley and J. Shi, "Diagnosis of multiple fixture faults in panel assembly," *ASME J. Manufact. Sci. Eng.*, vol. 120, pp. 793–801, 1998.
- [9] J. Shi and J. Jin, "Modeling and diagnosis for automotive body assembly process using state space models," in *Proc. Int. Conf. Intelligent Manufacturing System*, Seoul, Korea, 1997, pp. 189–196.
- [10] J. Jin and J. Shi, "State space modeling of sheet metal assembly for dimensional control," *ASME J. Manufact. Sci. Eng.*, vol. 121, pp. 756–762, 1999.
- [11] R. Mantripragada and D. E. Whitney, "Modeling and controlling variation propagation in mechanical assemblies using state transition models," *IEEE Trans. Robot. Automat.*, vol. 15, pp. 124–140, Feb. 1999.
- [12] Y. Ding, D. Ceglarek, and J. Shi, "Modeling and diagnosis of multistage manufacturing processes: Part I state space model," in *Proc. Japan/USA Symp. Flexible Automation*, Ann Arbor, MI, July 23–26, 2000.
- [13] S. Zhou, Q. Huang, and J. Shi, "State space modeling of dimensional variation propagation in multistage machining process using differential motion vectors," *IEEE Trans. Robot. Automat.*, vol. 19, pp. 296–309, Feb. 2003.
- [14] Q. Huang, N. Zhou, and J. Shi, "Stream of variation modeling and diagnosis of multi-station machining processes," in *Proc. ASME International Mechanical Engineering Congr. Expo. (IMECE'00)*, vol. MED-11, Orlando, FL, Nov. 2000, pp. 81–88.
- [15] D. Djurdjanovic and J. Ni, "Linear state space modeling of dimensional machining errors," in *Trans. North Amer. Manufact. Res. Inst. SME*, vol. 29, 2001, pp. 541–548.
- [16] Y. Ding, D. Ceglarek, and J. Shi, "Fault diagnosis of multistage manufacturing processes by using state space approach," in *Trans. ASME, J. Manufact. Sci. Eng.*, vol. 124, 2002, pp. 313–322.
- [17] S. Zhou, Y. Ding, Y. Chen, and J. Shi, "Diagnosability study of multistage manufacturing process based on linear mixed-effects models," *Technometrics*, vol. 45, no. 4, pp. 312–325, 2003.
- [18] Y. Ding, J. Shi, and D. Ceglarek, "Diagnosability analysis of multi-station manufacturing processes," *Trans. ASME, J. Dyn. Syst. Meas. Control*, vol. 124, pp. 1–13, 2002.
- [19] Y. Ding, S. Zhou, and Y. Chen, "A comparison study of process variation estimators for in-process dimensional measurements and control," *Trans. ASME, J. Dyn. Syst. Meas. Control*, to be published.
- [20] *Handbook of Geometrical Tolerancing: Design, Manufacturing and Inspection*, Wiley, New York, 1995. G. Henzold.
- [21] W. J. Rugh, *Linear System Theory*. New York: Prentice-Hall, 1996.
- [22] R. G. Brown and P. Y. C. Hwang, *Introduction to Random Signals and Applied Kalman Filtering*. New York: Wiley, 1997.
- [23] R. H. Myers, *Classical and Modern Regression with Applications*. Pacific Grove, CA: Brooks/Cole, 1990.
- [24] L. El Ghaoui and G. Calafiore, "Robust filtering for discrete-time systems with bounded noise and parametric uncertainty," *IEEE Trans. Automat. Contr.*, vol. 46, pp. 1084–1089, July 2001.
- [25] G. Calafiore and L. El Ghaoui, "Robust maximum likelihood estimation in the linear model," *Automatica*, vol. 37, no. 4, pp. 573–580, 2001.
- [26] C. R. Rao and J. Kleffe, *Estimation of Variance Components and Applications*. Amsterdam, The Netherlands: North-Holland, 1988.
- [27] S. R. Searle, G. Casella, and C. E. McCulloch, *Variance Components*. New York: Wiley, 1992.
- [28] C. R. Rao, "Estimation of variance components—MINQUE theory," *J. Multivariate Anal.*, vol. 1, pp. 257–275, 1971.
- [29] D. A. Harville, "Maximum likelihood approaches to variance component estimation and to related problems," *J. Amer. Stat. Assoc.*, vol. 72, no. 358, pp. 320–338, 1977.
- [30] C. R. Rao, "Estimation of variance and covariance components in linear models," *J. Amer. Stat. Assoc.*, vol. 67, pp. 112–115, 1972.
- [31] H. White, *Asymptotic Theory for Econometricians*. New York: Academic, 1984.
- [32] B. Seifert, "Testing hypotheses in linear mixed models," *J. Stat. Planning Inference*, vol. 36, pp. 253–268, 1993.
- [33] A. I. Khuri, T. Mathew, and B. K. Sinha, *Statistical Tests for Linear Mixed Models*. New York: Wiley, 1998.
- [34] C. McCulloch and S. R. Searle, *Generalized, Linear, and Mixed Models*. New York: Wiley, 2001.
- [35] B. Seifert, "Exact tests in unbalanced mixed analysis of variance," *J. Stat. Planning Inference*, vol. 30, pp. 257–266, 1992.
- [36] J. Kleffe and B. Seifert, "On the role of MINQUE in testing of hypotheses under linear mixed models," *Comm. Stats. Theory Meth.*, vol. 17, pp. 1287–1309, 1988.
- [37] S. E. Stern and A. H. Welsh, "Likelihood inference for small variance components," *Canad. J. Stat.*, vol. 28, no. 3, pp. 517–532, 2000.
- [38] B. Seifert, "Estimation and test of variance components using the MINQUE-method," *Statistics*, vol. 16, no. 4, pp. 621–635, 1985.